

MODELING OF CONFORMATIONAL CHANGES OF POLYELECTROLYTES ON THE SURFACE OF A TRANSVERSELY POLARIZED METAL NANOWIRE IN AN EXTERNAL ELECTRIC FIELD

Kucherenko M.G., Kruchinin N.Yu.* , Neyasov P. P.

Center of Laser and Informational Biophysics, Orenburg State University, Orenburg, Russia, clibph@yandex.ru,
kruchinin_56@mail.ru

Gold nanowires with polyelectrolytes adsorbed on their surface are widely used in various biomedical research. In this work, for the first time, conformational changes in polyelectrolytes on the surface of a gold nanowire transversely polarized in an external electric field were considered. The properties of a specially created analytical model of conformational rearrangements of a Gaussian macromolecular chain adsorbed on the surface of a cylindrical metal nanowire in an external electric field transverse to the axis of the nanowire were investigated. Conformational changes of uniformly charged polypeptides on the surface of a transversely polarized gold nanowire have been studied using molecular dynamics simulation. On the basis of the analytical model and the results of molecular dynamics simulation, the spatial distributions of the density of polyelectrolyte units on the surface of the nanowire were constructed. With an increase in the strength of the external electric field, an asymmetric stretching of the polyelectrolyte fringe in the direction of the dipole moment of the transversely polarized nanowire was observed.

Keywords: metal nanowire, polyelectrolyte, conformational changes, molecular dynamics

Introduction

Plasmonic nanorods and nanowires with polymer molecules adsorbed on their surface are widely used for biological nanoprobe based on the effect of surface-enhanced Raman scattering, as well as for creating various chemical sensors [1–7]. In this case, of particular interest is the control of conformational changes in adsorbed macrochains under the influence of an external electric field in order to create similar nanoprobe and sensors with controlled characteristics [8–14].

Previously, the authors studied electrically induced conformational changes in macromolecular chains on the surface of gold nanoobjects of spherical [15–17] and cylindrical [18–20] shapes, as well as on the surface of gold prolate nanospheroids [21–23] and the flat surface of a gold crystal. It was shown that under the influence of both a static external electric field and microwave electromagnetic radiation, the conformational structure of polyelectrolyte chains adsorbed on the surface of metal nanoobjects changes significantly, and at the same time depends on the shape of the nanoobject. At the same time, it is of interest to study conformational changes in polyelectrolytes with a uniform distribution of charges of the same sign along the entire macrochain on the surface of a metal cylindrical nanowire or nanorod polarized in the transverse direction in a static electric field, which was not disclosed in previously published works [18–20].

Therefore, the purpose of this work is to study the conformational changes of uniformly charged polyelectrolytes on the surface of a metal nanowire transversely polarized in an external electric field. For this, two approaches will be used: a statistical description of the macromolecular fringe layer and molecular dynamics (MD) simulation.

1 Formation of a macromolecular fringe layer on the surface of a cylindrical nanowire: a mathematical model

1.1 Mathematical model of formation of the fringe layer of a polyelectrolyte macromolecular chain on the surface of a transversely polarized nanowire

A change in the conformations of macrochains of a polyelectrolyte adsorbed on a nanowire can be carried out by an external electric field that polarizes the conductor. In the simplest model, polymer molecules are represented as ideal Gaussian chains, but the attraction of links to the surface of the adsorbent

is taken into account. The intensity of the quasi-static field outside the cylinder of radius R , i.e. when $r > R$ and placed in the field \mathbf{E}_0 has the form [24] ($\mathbf{n}_x, \mathbf{n}_y$ are the unit vectors of the Cartesian coordinate system)

$$\mathbf{E}_2(r, \varphi) = E_0 \mathbf{n}_x + E_0 \frac{\varepsilon_1(\omega) - \varepsilon_2}{\varepsilon_1(\omega) + \varepsilon_2} \frac{R^2}{r^2} \left[(1 - 2 \sin^2 \varphi) \cdot \mathbf{n}_x + \sin 2\varphi \cdot \mathbf{n}_y \right]. \quad (1)$$

The adsorption potential of the surface of a circular nanowire in the case of van der Waals adsorption can be effectively represented by a combination of the simplest model potentials “solid wall–delta functional well”: $V_1(r) = V_\infty(R) - \alpha \delta(r - r_0)$ [18]. When a nanowire is placed in a uniform electric field, its potential becomes dependent on the angular variable φ in the cross-sectional plane as a result of conductor polarization. Then the potential of the total field in the space outside the nanowire with the polarized component $\mathbf{E}_x(t)$ can be written as the sum

$$V(\mathbf{r}) = V_1(r) + V_2(r, \varphi) = V_\infty(R) - \alpha \delta(r - r_0) - eE_0 r \cos \varphi + V_p(r, \varphi), \quad (2)$$

where

$$V_2(r, \varphi) = -eE_0 r \cos \varphi + \frac{\varepsilon_1(\omega) - \varepsilon_2}{\varepsilon_1(\omega) + \varepsilon_2} R^2 eE_0 \frac{\cos \varphi}{r} \quad (3)$$

– the energy of interaction of a polyelectrolyte unit carrying a charge e with the primary external electric field and the polarization field of the wire. The dielectric constants $\varepsilon_1(\omega), \varepsilon_2$ in (3) characterize the nanowire metal and the environment, respectively.

To study the spatial structure of the macrochain, a conformational function $\psi(\mathbf{r})$ is introduced that satisfies a Schrodinger-type differential equation [25]

$$\frac{a^2 kT}{6} \nabla^2 \psi(\mathbf{r}) = [V(\mathbf{r}) - \varepsilon] \psi(\mathbf{r}), \quad (4)$$

where a is the size of the chain link; T is the temperature of the colloidal solution. In the case of a sufficiently weak external field, potential (3) can be taken into account in the framework of perturbation theory. Equation (4) with potential (2) contains an angular variable, so it should be written in the form

$$\frac{a^2 kT}{6} \left[\frac{1}{r} \frac{\partial}{\partial r} r \frac{\partial}{\partial r} + \frac{1}{r^2} \frac{\partial^2}{\partial \varphi^2} \right] \psi(\mathbf{r}) = [V(\mathbf{r}) - \varepsilon] \psi(\mathbf{r}). \quad (5)$$

Solution (5) can be represented as $\psi(\mathbf{r}) = F(r) \Phi_m(\varphi)$, where $\Phi_m(\varphi)$ is the eigenfunction of the projection operator of the quantum orbital angular momentum with integer m : $\Phi_m(\varphi) = 1/\sqrt{2\pi} \exp(im\varphi)$.

For the radial function $F_m(r)$ (5), we obtain the equation [19]

$$\frac{a^2 kT}{6} \left[\frac{1}{r} \frac{d}{dr} r \frac{d}{dr} - \frac{m^2}{r^2} \right] F_m(r) = [V(r) - \varepsilon_m] F_m(r). \quad (6)$$

Here in (6) the radial potential $V(r) = V_1(r) + V_2(r)$, and $V_2(r)$ is defined by the relation $V_2(r, \varphi) = V_2(r) \Phi_1(\varphi)$, or

$$V_2(r, \varphi) = - \left[1 - \alpha'(\omega) \left(\frac{R}{r} \right)^2 \right] r E_0 \cos \varphi$$

$$V_2(r, \varphi) = -eE_0 r \cos \varphi + \frac{\varepsilon_1(\omega) - \varepsilon_2}{\varepsilon_1(\omega) + \varepsilon_2} R^2 eE_0 \frac{\cos \varphi}{r}$$

The equation for the function $F_m(r)$ without taking into account the polarization part $V_2(r)$ of the potential is obtained from (5), and can be written in the form

$$F_m''(r) + \frac{1}{r} F_m'(r) - \frac{m^2}{r^2} F_m(r) = \frac{6}{a^2 kT} [V_1(r) - \varepsilon_m] F_m(r). \quad (7)$$

In the absence of a potential $V_1(r) = V_\infty(R) - \alpha \delta(r - r_0)$, equation (7) is the Bessel equation for cylindrical functions $Z_m(\xi)$. Thus, the solution to (7) are the Bessel functions of the imaginary argument $I_m(q_m r)$ и $K_m(q_m r)$, $\xi = q_m r$, $q_m^2 = -\frac{6\varepsilon_m}{a^2 kT}$. Then, as solutions of equation (4) with a certain index m in the field $V(r) = V_1(r)$, decaying at infinity, we can write the following expressions

$$\begin{cases} F_m^I(r) = A_m I_m(q_m r) + B_m K_m(q_m r), & R < r < r_0 \\ F_m^{II}(r) = C_m K_m(q_m r), & r_0 < r < \infty \end{cases}. \quad (8)$$

The constants A_m , B_m and C_m are found from the following boundary conditions and conjugation conditions that the functions $\psi(r)$ must satisfy

$$\psi_I(R) = 0, \quad \psi_I(r_0) = \psi_{II}(r_0), \quad \psi_{II}'(r_0) - \psi_I'(r_0) = -\frac{6\alpha}{a^2 kT} \psi_{II}(r_0). \quad (9)$$

The last equation in (9) allows us to determine the only discrete level of the spectrum ε_m for each integer index m [19]. For $m=0$, we arrive at the problem with circular symmetry of the distribution density $n(r) = \psi^2(r)$ of links, which we have already studied earlier in a number of papers.

In the general case of an arbitrary index m , to determine the parameters q_m and ε_m it is necessary to use the equation

$$\frac{d}{dr} F_m^{II}(r)|_{r=r_0} - \frac{d}{dr} F_m^I(r)|_{r=r_0} = -\frac{6\alpha}{a^2 kT} F_m^{II}(r_0), \quad (10)$$

and from the other two equalities (9) there are relations between the constants A_m and two other constants B_m and C_m .

Then solutions (8) take the form

$$\begin{cases} F_m^I(r) = A_m \left[I_m(q_m r) - \frac{I_m(q_m R)}{K_m(q_m R)} K_m(q_m r) \right], & R < r < r_0 \\ F_m^{II}(r) = A_m \left[\frac{I_m(q_m r_0)}{K_m(q_m r_0)} - \frac{I_m(q_m R)}{K_m(q_m R)} \right] K_m(q_m r), & r_0 < r < \infty \end{cases}. \quad (11)$$

Substituting (11) into (10) we obtain the general transcendental equation for the eigenvalues q_m

$$\frac{a^2 kT}{6\alpha r_0} = I_m(q_m r_0) K_m(q_m r_0) - K_m^2(q_m r_0) \frac{I_m(q_m R)}{K_m(q_m R)}. \quad (12)$$

It was shown in [19] that the functions (11) with $m=0$ and $m=1$ are especially important for constructing the first-order perturbation theory. In this case, the density $n(r, \varphi) = \psi^2(r, \varphi)$ of links of the adsorbed macrochain will still be determined by functions (8) or (11) with index $m=0$, and eigenvalues ε_0 . The first-order corrections to the eigenvalue ε_0 , when perturbations $V_2(r, \varphi) = -eE_0 r \cos \varphi + V_p(r, \varphi)$ are taken into account, are equal to zero for states (8) or (11) [19]. However, the correct use of the Rayleigh-Schrodinger perturbation theory requires taking into account states (11) with $m=1$ to clarify the basic states $F_0^I(r), F_0^{II}(r)$ in the field of a polarized nanowire.

1.2 Calculations based on the conformational model of an adsorbed Gaussian chain on the surface of a transversely polarized nanowire

Based on the results of calculations using formulas (1)–(12), spatial distributions of the density of polyelectrolyte units on the surface of a transversely polarized metal nanowire were constructed. All link density distributions are presented normalized to the value of the local density maximum.

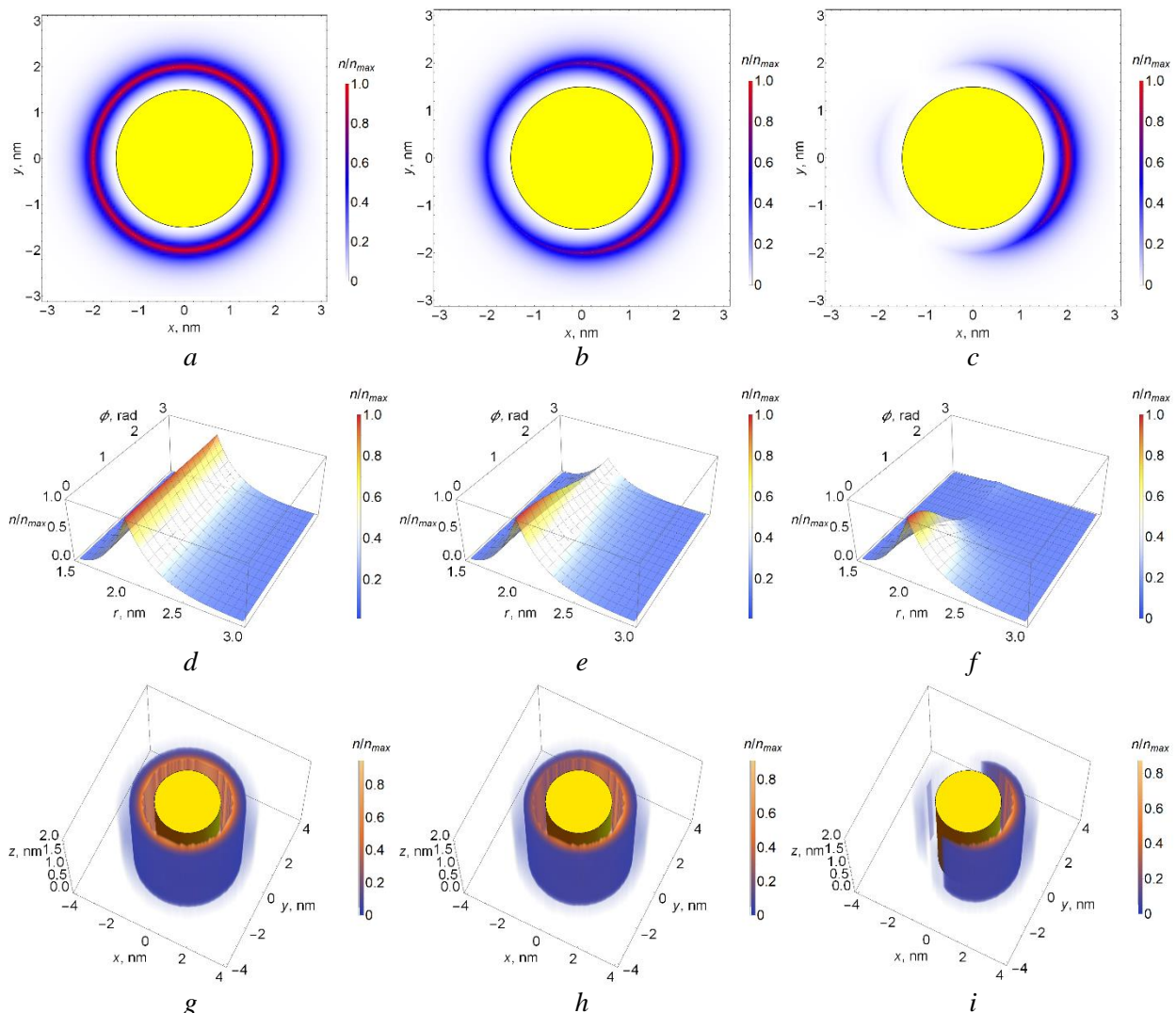


Fig. 1. Spatial distributions of the density of polyelectrolyte units on the surface of a transversely polarized nanowire at different external electric field strengths E_0 (directed along the x axis): 10^4 (a, d, g), 10^5 (b, e, h), 10^6 V/cm (c, f, i). Other parameters: $e' = -0.1 |e|$, $R = 1.5$ nm, $r_0 = 2$ nm, $\alpha = 5 \cdot 10^{-3}$ eV·nm, $T = 300$ K, $a = 0.5$ nm.

Figure 1 shows the spatial distributions of the density of polyelectrolyte units at different external electric field strengths E_0 : 10^4 (Fig. 1a, 1d and 1g), 10^5 (Fig. 1b, 1e and 1h) and 10^6 V/cm (Fig. 1c, 1f and 1i). In this case, the following parameters were set in expressions (1-14): link charge $e' = -0.1 |e|$, nanowire

radius $R=1.5$ nm, location of the potential well from the nanowire axis $r_0=2$ nm, potential well depth $\alpha=5\cdot 10^{-3}$ eV·nm, temperature $T=300$ K and link size $a=0.5$ nm. As can be seen from Figures 1a–1c, with an increase in the strength of the electric field directed from left to right, the links of the polyelectrolyte macrochain are shifted to the right positively charged region of the transversely polarized metal nanowire. At a low electric field strength, the polyelectrolyte almost uniformly envelops the nanowire (Figs. 1a, 1d, and 1g). At the same time, the higher the electric field strength, the stronger the differences in the density of polyelectrolyte units over the cross section of the nanowire (Fig. 1d-1f) for fields of different strengths, and the more the edge of the macrochain shifted to the positively charged region of the polarized nanowire.

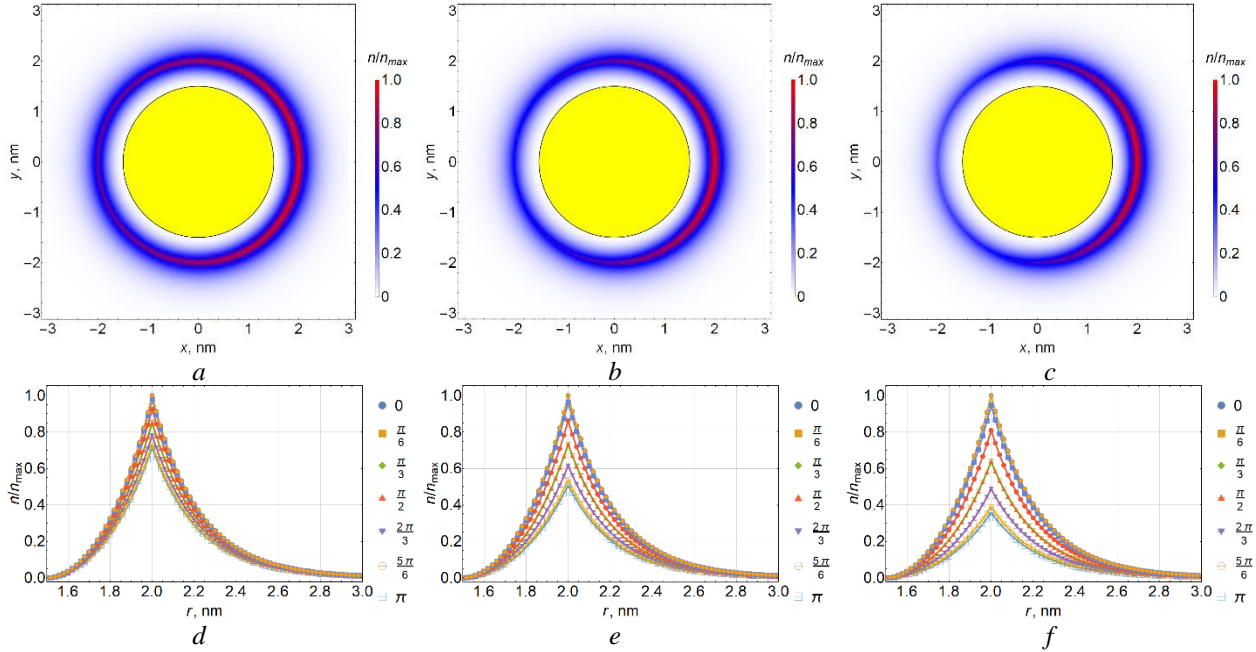


Fig. 2. Spatial distributions of the density of polyelectrolyte units on the surface of a transversely polarized nanowire at different charges of its unit e : - 0.05 (a, d), - 0.1 (b, e), - 0.15 $|e|$ (c, f) Other parameters: $R=1.5$ nm, $r_0=2$ nm, $\alpha=5\cdot 10^{-3}$ eV·nm, $T=300$ K, $a=0.5$ nm, $E_0=10^5$ V/cm (directed along the axis x).

Figure 2 shows the spatial distributions of the density of the polyelectrolyte units for different values of the charge of the polyelectrolyte unit: - 0,05 $|e|$ (Fig. 2a and 2d), - 0.1 $|e|$ (Fig. 2b and 2e) and - 0.15 $|e|$ (Fig. 2c and 2f) and a constant value of the external electric field $E_0=10^5$ V/cm. The following parameters were used in expressions (1)-(12): $R=1.5$ nm, $r_0=2$ nm, $\alpha=5\cdot 10^{-3}$ eV·nm, $T=300$ K, $a=0.5$ nm. It can be seen that as the charge of the polyelectrolyte link increases, the fragments of the macromolecule in the cross section of the nanowire are increasingly shifted towards the positively charged pole. At the same time, the density of macrochain links in the positively and negatively charged regions of the transversely polarized nanowire differs the more, the greater the absolute value of the charge of the polyelectrolyte link (Fig. 2d-e). This is due to the fact that with an increase in the absolute value of the macrochain charge, the electrostatic forces of interaction between the macromolecule and the polarized nanowire increase at a constant potential well depth α , which leads to a displacement of the edge of the charged polyelectrolyte into the oppositely charged region of the nanowire.

In addition, when modeling on the basis of expressions (1)–(12), the influence of variations of other theory parameters on the structural rearrangement of the fringe of a polyelectrolyte molecule adsorbed on the surface of a transversely polarized nanowire was estimated. Figure 3 shows the spatial distributions of the density of polyelectrolyte units at different temperatures: 250 (Fig. 3a), 300 (Fig. 3b) and 350 K (Fig. 3c) with unchanged parameters: $e'=-0.1$ $|e|$, $R=1.5$ nm, $r_0=2$ nm, $\alpha=5\cdot 10^{-3}$ eV·nm, $E_0=10^5$ V/cm, $a=0.5$ nm. It can be seen from the figure that, at a constant external electric field strength, an increase in the temperature of the colloid leads to the fact that the polyelectrolyte units move freely over the surface of the nanowire and the macrochain uniformly envelops the nanowire. This is due to the fact that the kinetic energy of the macrochain links exceeds the potential barriers caused by attraction to the surface of the nanowire. The same effect takes place when the depth of the potential well α decreases. Thus, when the depth of the potential well decreases from $6\cdot 10^{-3}$ eV·nm to $4\cdot 10^{-3}$ eV·nm and the values of the parameters in expressions (1)-(12)

equal to $e' = -0.1 |e|$, $R = 1.5$ nm, $r_0 = 2$ nm, $T = 300$ K, $E_0 = 10^5$ V/cm, $a = 0.5$ nm, the fringe around the nanowire also took a shape similar to the case of high temperature (Fig. 3c), i.e. uniformly enveloping the nanowire. The same effect was caused by a decrease in the nanowire radius from 1.7 nm to 1.3 nm or an increase in the link size from 0.45 nm to 0.55 nm with unchanged parameters: $e' = -0.1 |e|$, $\alpha = 5 \cdot 10^{-3}$ eV·nm, $T = 300$ K, $E_0 = 10^5$ V/cm.

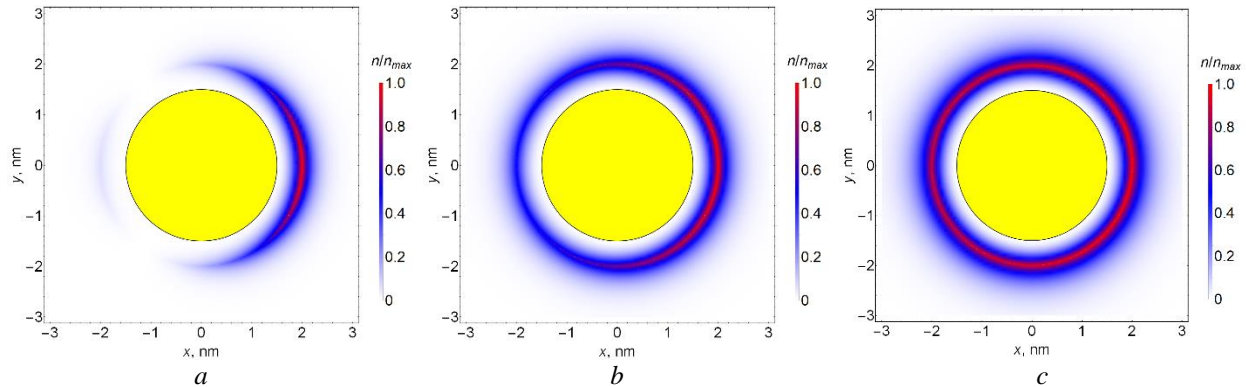


Fig. 3. Spatial distributions of the density of polyelectrolyte units on the surface of a transversely polarized nanowire at different temperatures T : 250 (a), 300 (b), 350 K (c) Other parameters: $e' = -0.1 |e|$, $R = 1.5$ nm, $r_0 = 2$ nm, $\alpha = 5 \cdot 10^{-3}$ eV·nm, $a = 0.5$ nm, $E_0 = 10^5$ V/cm (directed along the axis x).

2 Molecular dynamics simulation

In this work, MD simulation of uniformly charged polypeptides consisting of 800 amino acid residues was performed on the surface of a cylindrical gold nanowire polarized in the transverse direction in an external electric field. The model of a gold nanowire was obtained by cutting a cylinder with a radius of 1.5 nm and a length of 15.5 nm from a gold crystal, and its atoms remained fixed during the MD simulation.

The following negatively charged polypeptides have been considered:

- 1) polypeptide $(A_{10}DA_9)_{40}$, consisting of 760 Ala units (A, neutral) with uniformly distributed 40 Asp units (D, charge $-1e$), the total macrochain charge was $-40e$;
- 2) polypeptide $(A_5DA_4)_{80}$, consisting of 720 Ala units with 80 Asp units uniformly distributed (total macrochain charge $-80e$);
- 3) polypeptide $(A_2DA_2)_{160}$, consisting of 640 Ala units with 160 Asp units uniformly distributed (total macrochain charge $-160e$).

MD simulation was performed using the NAMD 2.13 software package [25]. For polypeptides, the CHARMM22 force field was used [27]. Non-covalent interactions with a gold nanowire were described by the Lennard-Jones potential parameterized in [28]. The Van der Waals potential was cut off at a distance of 1.2 nm using a smoothing function between 1.0 and 1.2 nm. Electrostatic interactions were calculated directly at a distance of 1.2 nm, and at greater distances, we used Ewald's particle-mesh approach (PME) [29] with a grid step of 0.11 nm. The entire nanosystem was placed in a cube with 24 nm edges filled with TIP3P water molecules [30]. To control the obtaining of equilibrium conformations, the change in the root-mean-square distance between polypeptide atoms in different conformations (RMSD) was monitored. MD simulation was performed at a constant temperature at 900 K with a subsequent reduction to 300 K.

First, such conformational structures of macrochains were obtained, in which the polypeptide enveloped the surface of the nanowire. For this purpose, MD simulation of negatively charged polypeptides on the surface of a positively charged gold nanowire (surface charge density $+3.3e/\text{nm}^2$) was carried out. Three starting conformational structures of each polypeptide were obtained for MD simulation on the surface of a transversely polarized gold nanowire.

If the external electric field vector is directed transversely with respect to the axis of a cylindrical metal nanowire, then electric charges will be induced on the surface of the nanowire with a surface density proportional to the cosine of the angle between the directions of the electric field vectors \mathbf{E} and the normal to the surface [31]:

$$\sigma = \frac{E}{2\pi} \cos \theta \quad (13)$$

Therefore, the local electric field of a nanowire polarized in the transverse direction was set by assigning partial charges to nanowire atoms located on its surface according to the cosine law (13). The following values of the induced dipole moment of the nanowire per unit of its length were obtained: 0.75, 1.5, and 3 kD/nm. In this case, on the surface of the nanowire, the maximum value of the induced partial charge of the atom in the positively charged region of the polarized nanowire was $+0.125e$, $+0.25e$, and $+0.5e$, respectively.

2.1 MD simulation results

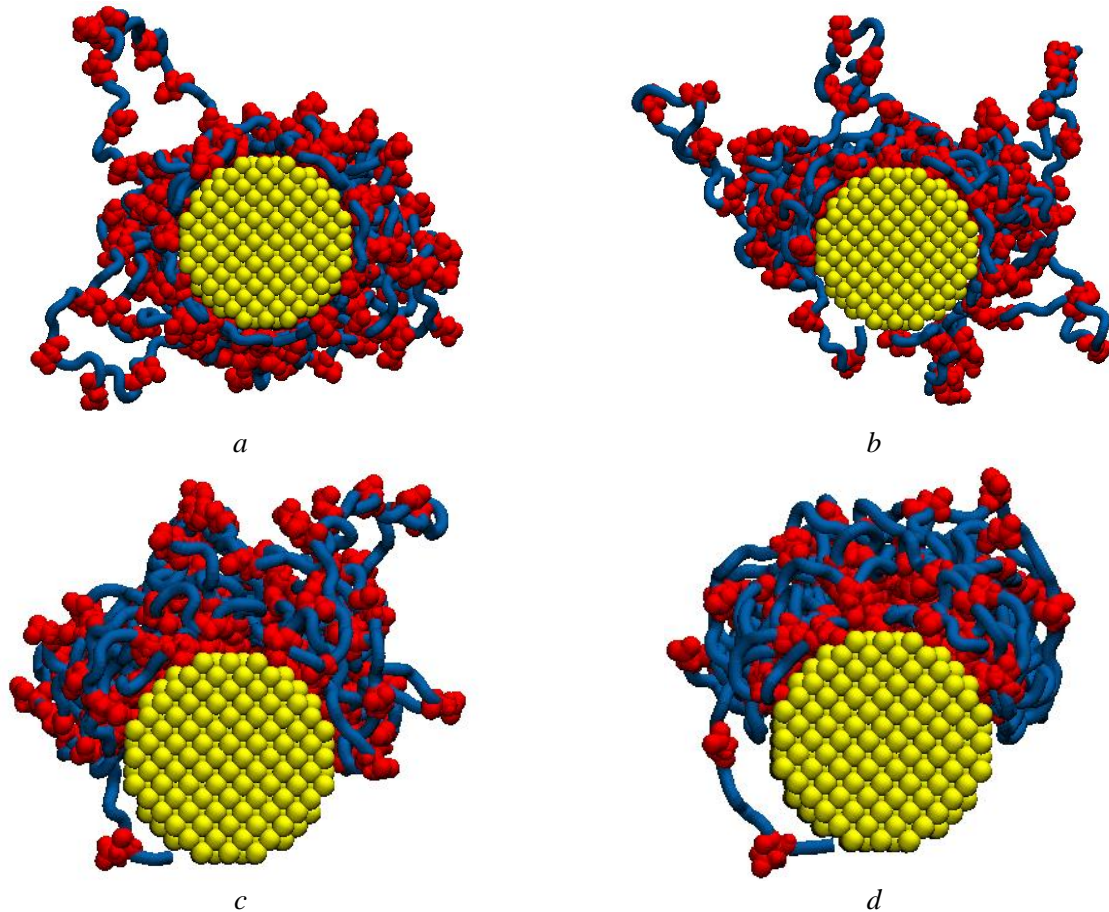


Fig. 4. Polypeptide $(A_2DA_2)_{160}$ in the starting conformation (a), as well as on the surface of a transversely polarized gold nanowire with a dipole moment (directed upwards): 0.75 (b), 1.5 (c) and 3 (d) kD/nm (the blue tube and red symbols denote Ala and Asp residues, respectively).

Figure 4a shows the starting conformational structure of the $(A_2DA_2)_{160}$ polypeptide, which was obtained at the end of MD simulation on a positively charged nanowire, with the macromolecular chain as a whole uniformly enveloping the nanowire. Figures 4b–4d show that as the dipole moment of the nanowire increases in the transverse direction, the macromolecular chain shifts more and more to the positively charged region of the nanowire (in the upper half of the cross section). At the maximum value of the dipole moment of the nanowire (Fig. 4d), almost all amino acid residues are located in the upper positively charged region of the nanowire. An exception is the only positively charged N-terminus of the polypeptide, which remained in the negatively charged region of the nanowire. A similar picture of displacement of negatively charged macrochain units to the positively charged region of the transversely polarized nanowire was observed for polypeptides $(A_{10}DA_9)_{40}$ and $(A_5DA_4)_{80}$.

Figure 5 shows the average angular dependences of the distribution of atoms of the polypeptide $(A_2DA_2)_{160}$, which were calculated with a step of 10 degrees along the cross section (a negatively charged pole in the nanowire cross section corresponds to an angle of 180 degrees, and a positively charged pole corresponds to an angle of 0 degrees). This figure shows that, in the starting conformation (curve 1), a generally uniform distribution of atoms of uniformly charged polypeptides around the nanowire is observed. At the value of the dipole moment of the nanowire equal to 0.75 kD/nm, a small part of the polypeptide

atoms shifted to the positively charged region of the nanowire (curve 2), and already at the value of the dipole moment of the nanowire equal to 1.5 kD/nm (curve 3), most of the amino acid residues of the polypeptide shifted to the positively charged region. Similar mean angular distributions of atoms were also observed for other considered polypeptides.

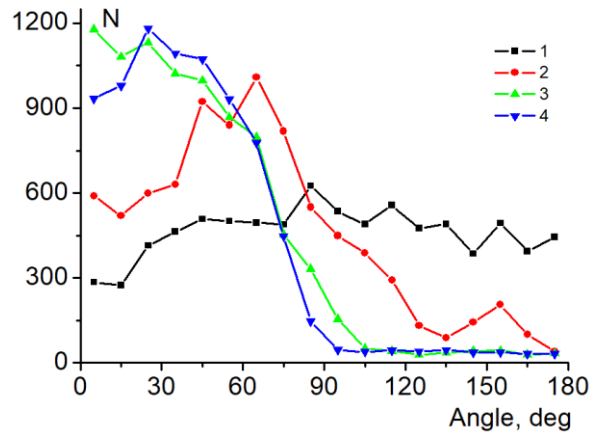


Fig. 5. Average angular dependences of the distribution of atoms of the polypeptide $(A_2DA_2)_{160}$ on the surface of a transversely polarized gold nanowire. In the figure, the numbers denote the values of the dipole moment of the nanowire: 1) – 0, 2) – 0.75, 3) – 1.5 and 4) – 3 kD/nm.

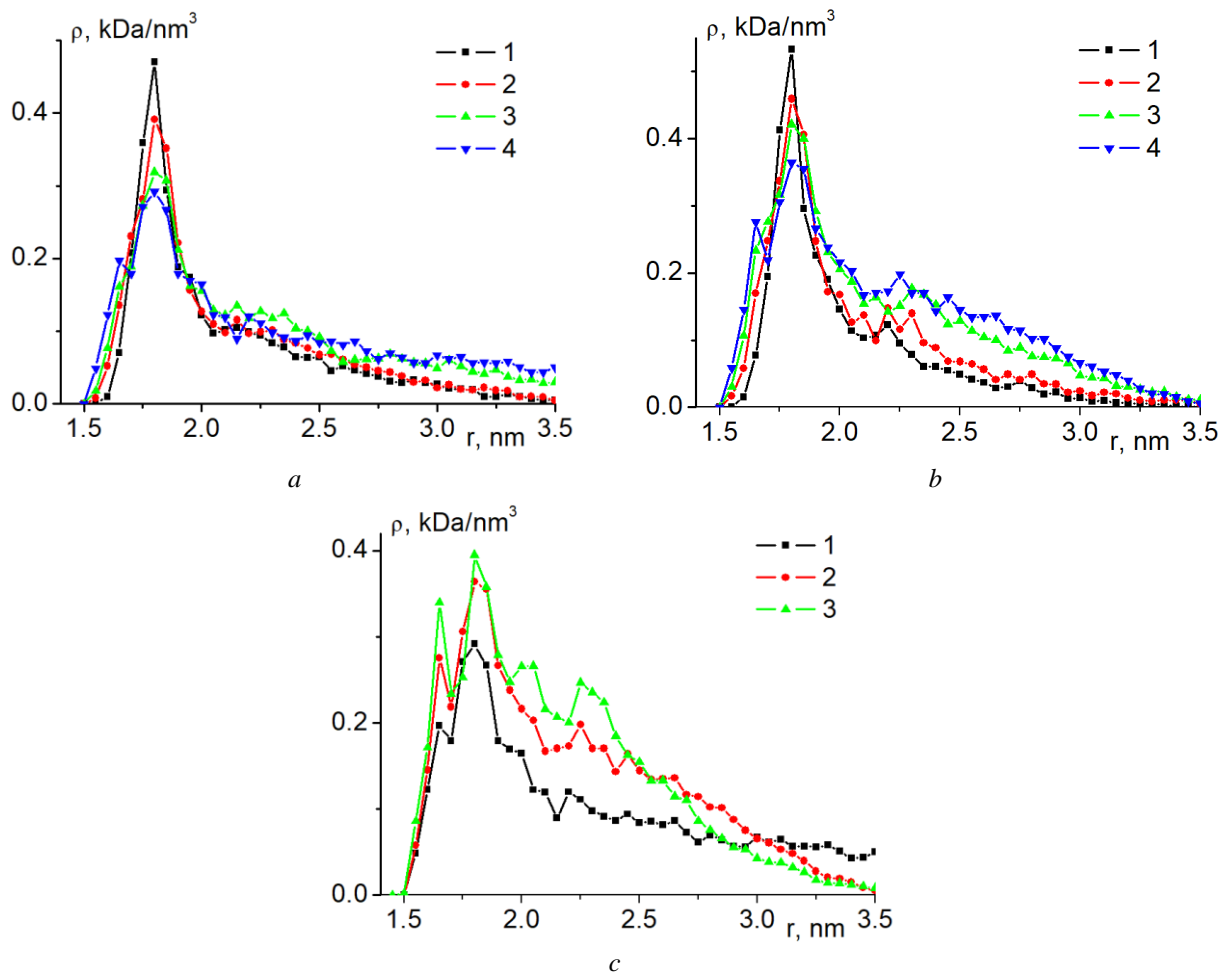


Fig. 6. Radial dependences of the average density of atoms of the polypeptide $(A_{10}DA_9)_{40}$ (a) and $(A_5DA_4)_{80}$ (b) on the surface of the positively charged half of the transversely polarized nanowire at dipole moment values: 1) – 0, 2) – 0.75, 3) – 1.5 and 4) – 3 kD/nm. Radial dependences of the average atomic density of polypeptides $(A_{10}DA_9)_{40}$ (c, 1), $(A_5DA_4)_{80}$ (c, 2), and $(A_2DA_2)_{160}$ (c, 3) on the surface of a positively charged region of a transversely polarized gold nanowire at a dipole moment of 3 kD/nm.

Figure 6 shows the radial dependences of the average density of polypeptide atoms on the surface of a positively charged region of a transversely polarized nanowire for various values of its dipole moment. It can be seen that as the dipole moment of the transversely polarized nanowire increases (Figs. 6a and 6b), the density of polypeptide atoms near the surface decreases more and more. This is due to the fact that when similarly charged units are displaced to the upper region and, accordingly, their number increases there, the polyelectrolyte fringe swells due to bulk interactions between macromolecule units. It is also seen in Fig. 3c that at the maximum value of the dipole moment of the nanowire considered for the polypeptide $(A_{10}DA_9)_{40}$ with the lowest density of charged units per macrochain length unit, the curve of the radial dependence of the density of polypeptide atoms is significantly lower than for the other two polypeptides. This is due to the fact that with an increase in the number of charged units per unit length of the polypeptide, the force of electrostatic attraction between the positively charged region of the transversely polarized nanowire and the negatively charged polypeptide increases.

Conclusion

Based on the expressions of the analytical model for the formation of a macromolecular fringe layer on the surface of a cylindrical metal nanowire, the conformational changes in the uniformly charged polyelectrolyte adsorbed on it under the action of a transversely directed external electric field were calculated. As the strength of the external electric field increased, an asymmetric stretching of the polyelectrolyte fringe was observed in the direction of the dipole moment of the transversely polarized nanowire. In this case, the links of the macrochain of the charged polyelectrolyte shifted to the oppositely charged pole along the cross section of the nanowire, and the like-charged pole became exposed relative to the charged macromolecule. An increase in the macrochain charge per unit of its length at a constant strength of the external transverse electric field led to an ever greater displacement of the polyelectrolyte fringe into the oppositely charged region of the transversely polarized nanowire. The influence of other parameters included in the obtained expressions of the mathematical model on changes in the polymer fringe of the adsorbed polyelectrolyte of the transversely polarized nanowire was evaluated. An increase in temperature, a decrease in the depth of the potential well, a decrease in the nanowire radius, and an increase in the link size led to the fact that the asymmetry of the pattern for the polyelectrolyte fringe disappeared and the macromolecular chain uniformly enveloped the transversely polarized nanowire.

The obtained picture of the density distribution of macrochain units is in qualitative agreement with the conformational structures of uniformly charged polypeptides adsorbed on a gold, transversely polarized nanowire, which appear as a result of the performed MD simulation. In the case of MD simulation, the asymmetric stretching of the polypeptide fringe in the direction of the dipole moment of the transversely polarized nanowire also occurred. In this case, the higher the value of the dipole moment of the gold nanowire and the greater the number of charged amino acid residues of the same sign per unit length of the polypeptide, the stronger the macrochain shifted to the oppositely charged region of the transversely polarized nanowire. In this region of the nanowire, the macromolecular fringe gradually swelled due to bulk interactions between the charged units of the macromolecule.

The asymmetric stretching of the polyelectrolyte fringe with an increase in the strength of the external electric field is due to its effect on the charged links of the macrochain. Under the influence of an external force, which leads to a decrease in the possible conformations of the macrochain, elastic forces arise that prevent such a rearrangement of the macromolecule and are of an entropic nature [25]. As the possible conformations of a macromolecule decrease, its conformational entropy also decreases. With an increase in the strength of the external electric field, the forces acting on the charged macrochain increase, which begins to shift to the oppositely charged region of the transversely polarized nanowire. In this case, the elastic forces, which are of an entropic nature, prevent this and tend to return the shape of such a fringe that evenly envelops the nanowire. In MD simulation, in addition to the entropy factor, the shape of the polyelectrolyte fringe on the surface of the transversely polarized nanowire is also affected by the force factor associated with volumetric interactions of macromolecule units with each other.

Such a rearrangement of the conformational structure of adsorbed uniformly charged macromolecules adsorbed on the surface of a metal nanowire, which occurs under the influence of an external, transversely directed electric field, can find practical application in the creation of new or modification of existing bionanoprobes and sensors that based on the effect of surface-enhanced Raman scattering and are sensitive to exposure to an external electric field.

We can also note further prospects for such studies of conformational changes in adsorbed polyelectrolytes on the surfaces of gold nanoparticles. Of great interest, in addition to spherical [15–17] and cylindrical [18–20] nanoobjects, is the study of conformational rearrangements on the surface of spheroidal gold nanoparticles with different anisotropy in order to obtain nanosystems with tunable plasmon characteristics. On the surface of a prolate [21–23] or oblate spheroidal nanoparticle, both charged and polarized along the rotation axis, the distribution of electric charges differs significantly from the cases of charge distribution on the surface of polarized spherical or cylindrical nanoobjects. Such an inhomogeneous distribution of charges on the surface will lead to the fact that on the surface of both charged and placed in a static or alternating electric field nanospheroids, the polyelectrolyte fringe will have a unique shape, depending on the ratio between the lengths of the major and minor axes of the nanospheroids.

Acknowledgements

This work was supported by the Ministry of Science and Higher Education of the Russian Federation within the framework of project no. FSGU-2020-0003.

REFERENCES

- 1 Pardehkhorrām R., Alshawawreh F., Gonçalves V.R., et al. Gooding. functionalized gold nanorod probes: a sophisticated design of SERS immunoassay for biodetection in complex media. *Anal. Chem.*, 2021, Vol. 93, pp. 12954-12965. <https://doi.org/10.1021/acs.analchem.1c02557>.
- 2 Sankari S.S., Dahms H., Tsai M., et al. Comparative study of an antimicrobial peptide and a neuropeptide conjugated with gold nanorods for the targeted photothermal killing of bacteria. *Colloids and Surfaces B: Biointerfaces*, 2021, Vol. 208, pp. 112117. <https://doi.org/10.1016/j.colsurfb.2021.112117>.
- 3 Ferhan A.R., Hwang Y., Ibrahim M.S.B., et al. Ultrahigh surface sensitivity of deposited gold nanorod arrays for nanoplasmonic biosensing. *Applied Materials Today*, 2021, Vol. 23, pp. 101046. <https://doi.org/10.1016/j.apmt.2021.101046>.
- 4 Nguyen V., Li Y., Henry J., et al. Gold nanorod enhanced photoacoustic microscopy and optical coherence tomography of choroidal neovascularization. *ACS Appl. Mater. Interfaces*, 2021, Vol. 13, pp. 40214-10228. <https://doi.org/10.1021/acsami.1c03504>.
- 5 Sheng G., Ni J., Xing K., et al. Infection microenvironment-responsive multifunctional peptide coated gold nanorods for bimodal antibacterial applications. *Colloid and Interface Science Communications*, 2021, Vol. 41, pp. 100379. <https://doi.org/10.1016/j.colcom.2021.100379>.
- 6 Creyer M.N., Jin Z., Moore C., et al. Modulation of gold nanorod growth via the proteolysis of dithiol peptides for enzymatic biomarker detection. *ACS Appl. Mater. Interfaces*, 2021, Vol. 13, pp. 45236-45243. <https://doi.org/10.1021/acsami.1c11620>.
- 7 Dong X., Ye J., Chen Y., et al. Intelligent peptide-nanorods against drug-resistant bacterial infection and promote wound healing by mild-temperature photothermal therapy. *Chemical Engineering Journal*, 2022, Vol. 432, pp. 134061. <https://doi.org/10.1016/j.cej.2021.134061>.
- 8 Kyaw H.H., Boonruang S., Mohammed W.S., Dutta J. Design of electric-field assisted surface plasmon resonance system for the detection of heavy metal ions in water. *AIP Advances*, 2015, Vol. 5, pp. 107226. <https://doi.org/10.1063/1.4934934>.
- 9 Chen Y., Cruz-Chu E.R., Woodard J., et al. Electrically induced conformational change of peptides on metallic nanosurfaces. *ACS Nano*, 2012, Vol. 6, pp. 8847-8856. <https://doi.org/10.1021/nn3027408>.
- 10 Bekardb I., Dunstan D.E. Electric field induced changes in protein conformation. *Soft Matter*, 2014, Vol.10, pp. 431-437. <https://doi.org/10.1039/C3SM52653D>.
- 11 Wu X., Liu Z., Zhu W. External electric field induced conformational changes as a buffer to increase the stability of CL-20/HMX cocrystal and its pure components. *Materials Today Communications*, 2021, Vol. 26, pp. 101696. <https://doi.org/10.1016/j.mtcomm.2020.101696>.
- 12 Mayya K.S., Schoeler B., Caruso F. Preparation and organization of nanoscale polyelectrolyte-coated gold nanoparticles. *Advanced Functional Materials*, 2003, Vol. 13: pp. 183-188. <https://doi.org/10.1002/adfm.200390028>.
- 13 Dobrynin A.V., Rubinstein M. Theory of polyelectrolytes in solutions and at surfaces. *Progress in Polymer Science*, 2005, Vol. 30, pp. 1049-1118. <https://doi.org/10.1016/j.progpolymsci.2005.07.006>.
- 14 Chong G., Hernandez R. Adsorption dynamics and structure of polycations on citrate-coated gold nanoparticles. *The Journal of Physical Chemistry C*, 2018, Vol. 122, pp. 19962-19969. <https://doi.org/10.1021/acs.jpcc.8b05202>.
- 15 Kruchinin N.Yu., Kucherenko M.G. Conformational rearrangements of polyampholytic polypeptides on metal nanoparticle surface in microwave electric field: molecular-dynamics simulation. *Colloid Journal*, 2020, Vol. 82, pp. 392-402. <https://doi.org/10.1134/S1061933X20040067>.

16 Kruchinin N.Yu., Kucherenko M.G., Neyasov P.P. Conformational changes of uniformly charged polyelectrolyte chains on the surface of a polarized gold nanoparticle: molecular dynamics simulation and the theory of a Gaussian chain in a field *Russian Journal of Physical Chemistry A*, 2021, Vol. 95, pp. 362-371. <https://doi.org/10.1134/S003602442102014X>.

17 Kruchinin N.Yu. Molecular dynamics simulation of uniformly charged polypeptides on the surface of a charged metal nanoparticle in an alternating electric field *Colloid Journal*, 2021, Vol. 83, pp. 326-334. <https://doi.org/10.1134/S1061933X2102006X>.

18 Kruchinin N.Yu., Kucherenko M.G. Rearrangements in the conformational structure of polypeptides on the surface of a metal nanowire in rotating electric field: molecular dynamics simulation *Colloid Journal*, 2021, Vol. 83, pp. 79-87. <https://doi.org/10.1134/S1061933X20060083>.

19 Kruchinin N.Yu., Kucherenko M.G. Rearrangement of the conformational structure of polyampholytes on the surface of a metal nanowire in a transverse microwave electric field. *Eurasian Physical Technical Journal*, 2021, Vol.18, pp. 16-28. doi:10.31489/2021No1/16-28.

20 Kruchinin N.Yu., Kucherenko M.G. Rearrangements in the conformational structure of polyampholytic polypeptides on the surface of a uniformly charged and polarized nanowire: Molecular dynamics simulation. *Surfaces and Interfaces*, 2021, Vol. 27, pp. 101517. <https://doi.org/10.1016/j.surf.2021.101517>.

21 Kruchinin N.Yu., Kucherenko M.G. Molecular dynamics simulation of conformational rearrangements in polyelectrolyte macromolecules on the surface of a charged or polarized prolate spheroidal metal nanoparticle. *Colloid Journal*, 2021, Vol. 83, pp. 591-604. <https://doi.org/10.1134/S1061933X21050070>

22 Kruchinin N.Yu., Kucherenko M.G. Modeling the conformational rearrangement of polyampholytes on the surface of a prolate spheroidal metal nanoparticle in alternating electric field. *High Energy Chemistry*, 2021, Vol. 55, pp. 442-453. <https://doi.org/10.1134/S0018143921060084>.

23 Kruchinin N.Yu., Kucherenko M.G. Molecular dynamics simulation of the conformational structure of uniform polypeptides on the surface of a polarized metal prolate nanospheroid with varying pH. *Russian Journal of Physical Chemistry A*, 2022, Vol. 96, pp. 624-632. <https://doi.org/10.1134/S0036024422030141>.

24 Novotny L., Hecht B. *Principles of nanooptics*. 2006, Cambridge: Cambridge University Press. 564p.

25 Grosberg A.Y., Khokhlov A.R. *Statistical Physics of Macromolecules*. 1994, AIP Press, New York. 347p

26 Phillips J.C., Braun R., Wang W., et al. Scalable molecular dynamics with NAMD. *J Comput Chem*. 2005, Vol. 26, pp. 1781-1802. <https://doi.org/10.1002/jcc.20289>.

27 MacKerell A.D. Jr., Bashford D., Bellott M., et al. All-atom empirical potential for molecular modeling and dynamics studies of proteins *J. Phys. Chem. B*. 1998, Vol. 102, pp. 3586-3616. <https://doi.org/10.1021/jp973084f>.

28 Heinz H., Vaia R.A., Farmer B.L., Naik R.R. Accurate simulation of surfaces and interfaces of face-centered cubic metals using 12-6 and 9-6 Lennard-Jones potentials. *J. Phys. Chem. C*. 2008, Vol. 112, pp. 17281-17290. <https://doi.org/10.1021/jp801931d>.

29 Darden T., York D., Pedersen L. Particle mesh Ewald: An N·log(N) method for Ewald sums in large systems *J. Chem. Phys*. 1993, Vol. 98, pp. 10089-10092. <https://doi.org/10.1063/1.464397>.

30 Jorgensen W.L., Chandrasekhar J., Madura J.D., et al. Comparison of simple potential functions for simulating liquid water. *J. Chem. Phys*. 1983, Vol. 79, pp. 926-935. <https://doi.org/10.1063/1.445869>.

31 Landau L.D., Pitaevskii L.P., Lifshitz E.M. *Electrodynamics of Continuous Media*, 2nd Edition, Elsevier Ltd., 1984, 460 p.